Advances in the effective-potential Monte Carlo method

Dominic Acocella and George K. Horton
Serin Physics Laboratory, Rutgers–the State University, Piscataway, New Jersey 08855-0849

E. Roger Cowley
Department of Physics, Camden College of Arts and Sciences, Rutgers–the State University, Camden, New Jersey 08122-1205

(Received 1 November 1994)

We describe some advances made in the effective-potential Monte Carlo (EPMC) method. In particular, the effective potential has previously been evaluated by expanding the potential up to finite order; we show that the infinite series can be summed analytically. Previous work also included various forms of an isotropic approximation and the low-coupling approximation; we discard the former, but retain the latter. We compare our results for neon with previous work and find significant differences. We argue that the finite order EPMC method is now obsolete and that the present formalism supersedes it. Some computational aspects are also discussed.

I. INTRODUCTION

The problem of calculating the thermodynamics of quantum crystals is a difficult one. Several approximations are available; however, these are typically valid either in the high-temperature or low-temperature extremes. The Wigner expansion,[1] for example, is an expansion in $\hbar$ and thus is only accurate for nearly classical systems. Perturbation theory[2] is an expansion about equilibrium, which does not converge for systems with large thermal motion or large zero-point motion, and indeed may give imaginary phonon frequencies in extreme cases. Self-consistent theory[3] cures this problem, but it too becomes unreliable when mean-square displacements become too large.

A completely numerical evaluation of the quantum mechanical partition function should, in principle, present no problems. In practice, however, this is not the case. The path integral Monte Carlo (PIMC) method[4] starts from Feynman's path integral representation of the partition function,[5] which it evaluates numerically. The main problem with the PIMC method is that it can be extremely time consuming. In particular, low-temperature quantities that depend on fluctuations (such as the specific heat or bulk modulus) take too long to obtain accurately. The only PIMC calculations of solid neon we are aware of are due to Cuccoli *et al.*[6] and, to a lesser extent, to Liu *et al.*[7] None of these gives PIMC values for the specific heat or for the bulk modulus. We are aware of only one PIMC calculation for solid helium;[8] it gives the potential energy (with a large uncertainty) for two temperatures at the ground state volume, but does not give the kinetic energy, pressure, specific heat, or bulk modulus. However, there are quantum Monte Carlo calculations of the ground state energy.[9,10] The PIMC method is, of course, an active area of research.

This sets the stage for the effective-potential method. Like the PIMC method, it starts from the path integral representation of the partition function. It was introduced by Feynman[5] who chose a variational approach to evaluating the partition function. The novelty in the effective-potential method is in the choice of the trial potential. Feynman expanded the potential about the average point of each path, not about the initial point (with the expectation that this would better incorporate quantum effects) and replaced the expansion coefficients by variational parameters. In this first derivation, Feynman expanded the potential to zeroth order only; i.e., for each path with the same average point, the potential is constant. Thus, for each average point, we can evaluate the path integral since it is a free particle one. This leaves a classical partition function with an effective potential.

The effective-potential method was later improved independently by Giachetti and Tognetti[11] and by Feynman and Kleinert.[12] They proposed expanding the potential to second order. Since the solution to the path integral with a quadratic potential is known, the path integral can again be evaluated, leaving a classical partition function with a now improved effective potential.

Since then there has been much interest in this method. A multitude of applications can be found in the literature, ranging from single particles in potential wells,[13] to one-dimensional chains,[14] to three-dimensional crystals.[15,16] For a more complete list of applications, the reader is referred to the review article by Cowley and Horton.[17] In the one-particle application of Ref. 13, the effective-potential method and other approximation schemes are compared to exact numerical solutions, and it is found that the effective-potential method is the most reliable.

In the N-body problem, the classical integral is evaluated numerically and, in particular, in three dimensions it is evaluated by Monte Carlo simulations, hence the name effective-potential Monte Carlo (EPMC). However, the numerical evaluation proves to be too difficult, and approximations are necessary. In all the literature (see Ref. 17 for examples), we find a Taylor expansion of the

0163-1829/95/51(17)/11406(10)/$06.00

potential combined with an expansion about equilibrium, and we find the low-coupling approximation (LCA). The only exceptions are specific one-dimensional, integrable potentials. In all the three-dimensional applications, we find several forms of an isotropic approximation.[15,16] In this paper, we shall show that the results of the infinite Taylor series can be summed analytically, and that the isotropic approximation can be avoided. The LCA is the only approximation which must be retained. We shall show that this formulation of EPMC theory is more reliable than earlier, more approximate versions and that it is just as easy to evaluate.

The LCA is absolutely necessary to the success of the EPMC method as a practical tool. An EPMC calculation without it would take so long that it would be more cost effective to use the PIMC method. An EPMC calculation without the LCA is so difficult that a quantitative investigation of the LCA has never been done. We believe that this investigation is necessary for EPMC theory to be generally accepted by the physics community. We will present such an investigation in a subsequent paper. Even without the LCA, the full EPMC method has some fundamental deficiencies at low temperature, as well as numerical difficulties. We will also report on a study of these matters in the near future.

In Sec. II, we summarize the derivation of the effective potential and show in more detail how to avoid cutting off the Taylor expansion and how to sum the resulting infinite series. In Sec. III we discuss computational aspects of applying the EPMC method and show how easy and efficient the algorithm is. In Sec. IV, we present our results for a model of neon and compare with previous work, pointing out the large improvements made by our formulation of the effective potential.

II. FORMALISM

We start from the three-dimensional, N-particle path integral representation of the partition function[5] Z,

$$Z = \int d^{3N}r(0) \int_{\mathbf{r}(0)=\mathbf{r}(\beta\hbar)} \mathcal{D}^{3N}r(t)\, e^{-\frac{1}{\hbar}S[\mathbf{r}(t)]},$$

$$S = \int_0^{\beta\hbar} \left(\frac{1}{2}m\dot{\mathbf{r}}^2(t) + V(\mathbf{r}(t))\right) dt.$$

Here $\mathbf{r}(t)$ is a $3N$-dimensional coordinate. To evaluate Z numerically, the path integral Monte Carlo method approximates the action integral S by a sum with M terms. The path integral becomes a $3NM$-dimensional integral which is evaluated by Monte Carlo simulation. M is called the Trotter number. As the temperature approaches zero, $\beta\hbar \to \infty$ and we need a larger M to accurately calculate S. Therefore, low-temperature PIMC simulations become very time consuming.

The effective-potential Monte Carlo method also starts from the three-dimensional, N-particle path integral representation of the partition function. It was first proposed by Feynman[5] as a variational method for evaluating Z. Following Feynman, we expand $V(\mathbf{r}(t))$ not about $\mathbf{r}(0)$, but about $\bar{r}$ [the average point on the path $\mathbf{r}(t)$], with the expectation that this will better incorporate quantum fluctuations, and we replace the expansion coefficients by arbitrary parameters, taking care to preseve any symmetry properties. We expand the potential up to quadratic terms; the linear term may be discarded without affecting the final results since its effect can only be to redefine the constant term. The resulting nonlocal, quadratic trial potential V_0 is

$$V_0(\mathbf{r}) = W(\bar{r}) + \frac{1}{2}(\mathbf{r}-\bar{r})_i \Omega_{ij}(\bar{r})(\mathbf{r}-\bar{r})_j,$$

$$\bar{r} = \frac{1}{\beta\hbar}\int_0^{\beta\hbar} \mathbf{r}(t)\, dt,$$

where Ω_{ij} are the trial force constants and $\Omega_{ij} = \Omega_{ji}$, $i,j = 1,\ldots,3N$. Here we use the summation convention for repeated indices. Thus, for each $\bar{r}$, we have a set of $3N(3N+1)/2 + 1$ parameters. We shall often use the notation $I\alpha$ for i; $I = 1,\ldots,N$ is the atom number, and $\alpha = 1,2,3$ is the dimension number (i.e., x, y, or z). For an isotropic approximation, which we shall not use, we would assume $\Omega_{I\alpha,J\beta} = \Omega_{IJ}\delta_{\alpha\beta}$, as done in Ref. 15. The trial partition function is

$$Z_0 = \int d^{3N}r(0) \int_{\mathbf{r}(0)=\mathbf{r}(\beta\hbar)} \mathcal{D}^{3N}r(t)\, e^{-\frac{1}{\hbar}S_0[\mathbf{r}(t)]},$$

$$S_0 = \int_0^{\beta\hbar} \left(\frac{1}{2}m\dot{\mathbf{r}}^2(t) + V_0(\mathbf{r}(t))\right) dt.$$

The variational principle is based on the Jensen-Peierls[18] inequality

$$F \le F_0 + \langle V(\mathbf{r}(0)) - V_0(\mathbf{r}(0))\rangle_0. \tag{1}$$

Following Liu *et al.*,[15] we evaluate the right-hand side of (1) by first calculating, for an arbitrary function $A(\mathbf{r})$, the quantity A_0,

$$A_0 = Z_0\langle A(\mathbf{r}(0))\rangle_0 = \int d^{3N}r(0)\, A(\mathbf{r}(0)) \times \int_{\mathbf{r}(0)=\mathbf{r}(\beta\hbar)} \mathcal{D}^{3N}r(t)\, e^{-\frac{1}{\hbar}S_0[\mathbf{r}(t)]}. \tag{2}$$

Since the trial potential is quadratic, the path integral can be evaluated analytically. We first introduce the new variable $\mathbf{R}$ with the constraint that $\mathbf{R} = \bar{r}$ and replace $\bar{r}$ by $\mathbf{R}$ everywhere:

$$A_0 = \int d^{3N}R \int d^{3N}r(0)\, A(\mathbf{r}(0)) \int_{\mathbf{r}(0)=\mathbf{r}(\beta\hbar)} \mathcal{D}^{3N}r(t) \times e^{-\frac{1}{\hbar}S_0[\mathbf{r}(t)]}\delta\left(\mathbf{R} - \frac{1}{\beta\hbar}\int_0^{\beta\hbar}\mathbf{r}(t)dt\right).$$

We then Fourier transform $A(\mathbf{r}(0))$ and the δ function, make the appropriate change of variables, and let

$$U^T_{ai}\Omega_{ij}U_{jb} = m\omega_a^2\delta_{ab}. \tag{3}$$

U is the orthogonal matrix which diagonalizes Ω and

its index a represents the normal modes of the system. Changing to the basis of normal modes, the path integrations separate into the product of $3N$ forced harmonic oscillators [the forcing term coming from the δ-function constraint and $A(\mathbf{r}(0))$]. Carrying out the remaining integrations, we finally get

$$A_0 = \left(\frac{m}{2\pi\beta\hbar^2}\right)^{3N/2} \int d^{3N}R \left[\frac{f_a}{\sinh f_a}\right] \times J_A(\mathbf{R}) e^{-\beta W(\mathbf{R})},$$

$$J_A(\mathbf{R}) = \int d^{3N}\mu \left[\frac{e^{-\mu_a^2/\alpha_a}}{(\pi\alpha_a)^{1/2}}\right] A(\mathbf{R}+U\boldsymbol{\mu}),$$

$$\alpha_a = \frac{\beta\hbar^2}{2mf_a}\left(\coth f_a - \frac{1}{f_a}\right), \tag{4}$$

$$f_a = \frac{\beta\hbar\omega_a}{2}. \tag{5}$$

We use the convention that repeated indices are summed over, unless the term is enclosed in square brackets, in which case the repeated indices are multiplied over. When there is ambiguity, the summation or product will be indicated explicitly.

Letting $A = 1$ and $A = V - V_0$ in (2), we have, respectively,

$$F_0 = -\frac{1}{\beta}\ln Z_0 = -\frac{1}{\beta}\ln\left\{\left(\frac{m}{2\pi\beta\hbar^2}\right)^{3N/2} \times \int d^{3N}R \left[\frac{f_a}{\sinh f_a}\right] e^{-\beta W(\mathbf{R})}\right\}, \tag{6}$$

$$\langle V - V_0\rangle_0 = \frac{1}{Z_0}\left(\frac{m}{2\pi\beta\hbar^2}\right)^{3N/2} \int d^{3N}R \left[\frac{f_a}{\sinh f_a}\right] \times e^{-\beta W(\mathbf{R})}\left(K(\mathbf{R}) - W(\mathbf{R}) - \frac{m\alpha_a f_a^2}{\beta^2\hbar^2}\right), \tag{7}$$

where $K(\mathbf{R}) = J_V(\mathbf{R})$ and $J_{V_0}(\mathbf{R})$ was integrated:

$$K(\mathbf{R}) = \int d^{3N}\mu \left[\frac{e^{-\mu_a^2/\alpha_a}}{(\pi\alpha_a)^{1/2}}\right] V(\mathbf{R}+U\boldsymbol{\mu}), \tag{8}$$

$$J_{V_0} = W(\mathbf{R}) + \frac{m\alpha_a f_a^2}{\beta^2\hbar^2}.$$

At this point we apply the variational principle. We vary the functional parameters $W(\mathbf{R})$ and $\Omega_{ij}(\mathbf{R})$ so as to minimize the right-hand side of (1):

$$\frac{\delta}{\delta W(\mathbf{R})}\left(F_0 + \langle V - V_0\rangle_0\right) = K(\mathbf{R}) - W(\mathbf{R}) - \frac{m\alpha_a f_a^2}{\beta^2\hbar^2} = 0.$$

Thus, $W(\mathbf{R}) = K(\mathbf{R}) - m\alpha_a f_a^2/\beta^2\hbar^2$ and, substituting $W(\mathbf{R})$ into (7), $\langle V - V_0\rangle_0 = 0$. Hence, from (1) we have $F \le F_0$, where (6) now becomes

$$Z_0 = \left(\frac{m}{2\pi\beta\hbar^2}\right)^{3N/2} \int d^{3N}R\, e^{-\beta V_{\text{eff}}(\mathbf{R})}, \tag{9}$$

$$V_{\text{eff}}(\mathbf{R}) = K(\mathbf{R}) - \frac{m\alpha_a f_a^2}{\beta^2\hbar^2} + \frac{1}{\beta}\sum_a \ln\left(\frac{\sinh f_a}{f_a}\right). \tag{10}$$

We see that the result of this variation is to reduce the quantum mechanical partition function to one of classical form. This is one of the main advantages of the effective-potential method, since a classical partition function is much easier to evaluate than a quantum mechanical one. The quantum effects of the system are incorporated into the effective potential. It is useful to note that if $\mathbf{R}$ is equal to the equilibrium configuration, then the index a represents the $3N$ phonon modes of the system (i.e., the normal modes are plane waves), but that in an arbitrary configuration $\mathbf{R}$ (where there is no crystal symmetry) this is not true. Nevertheless, we shall call the terms $1/\beta\ln(\sinh f_a/f_a) - m\alpha_a f_a^2/\beta^2\hbar^2$ in V_{eff} the phonon terms. $K(\mathbf{R})$ will be called the smeared potential.

Variation of F_0 with respect to Ω_{ij} is done by variation with respect to ω_a and U_{ia} under the constraint that U remain orthogonal. We get

$$U_{ai}^T \tilde{K}_{ij} U_{jb} = m\omega_a^2\delta_{ab}, \tag{11}$$

$$\tilde{K}_{ij} = \tilde{K}_{I\alpha,J\beta} = \frac{\partial^2 K(\mathbf{R})}{\partial R_{I\alpha}\partial R_{J\beta}}. \tag{12}$$

Comparing with Eq. (3), we see that the result of this variation is $\Omega_{ij} = \tilde{K}_{ij}$.

Although we have a simple classical partition function, the effective potential (10) is too complicated to evaluate. In particular, the smeared potential K [Eq. (8)] must be evaluated. To do this $3N$-dimensional integral, we start by expanding $V(\mathbf{R}+U\boldsymbol{\mu})$ around $\mathbf{R}$. Specializing to a two-body potential,

$$V(\mathbf{R}) = \frac{1}{2}\sum_I \sum_{J\ne I} \phi(\mathbf{R}_I - \mathbf{R}_J), \tag{13}$$

$$\begin{aligned} K(\mathbf{R}) &= \frac{1}{2}\sum_{I\ne J}\int d^{3N}\mu \left[\frac{e^{-\mu_a^2/\alpha_a}}{(\pi\alpha_a)^{1/2}}\right] \times\phi\left((\mathbf{R}+U\boldsymbol{\mu})_{I\gamma} - (\mathbf{R}+U\boldsymbol{\mu})_{J\gamma}\right) \\ &= \frac{1}{2}\sum_{I\ne J}\int d^{3N}\mu \left[\frac{e^{-\mu_a^2/\alpha_a}}{(\pi\alpha_a)^{1/2}}\right] \sum_{l=0}^{\infty}\frac{1}{l!} \times \left.\frac{\partial^l\phi(\mathbf{x})}{\partial x_{\gamma_1}\cdots\partial x_{\gamma_l}}\right|_{\mathbf{x}=\mathbf{R}_I-\mathbf{R}_J} (U_{I\gamma_1,a_1} - U_{J\gamma_1,a_1})\mu_{a_1} \\ &\quad \times\cdots(U_{I\gamma_l,a_l} - U_{J\gamma_l,a_l})\mu_{a_l} \\ &= \frac{1}{2}\sum_{I\ne J}\sum_{l=0}^{\infty}\frac{1}{l!}\frac{\partial^l\phi(\mathbf{R}_I-\mathbf{R}_J)}{\partial x_{\gamma_1}\cdots\partial x_{\gamma_l}} \times(U_{I\gamma_1,a_1} - U_{J\gamma_1,a_1})\cdots(U_{I\gamma_l,a_l} - U_{J\gamma_l,a_l}) \\ &\quad \times\int d^{3N}\mu \left[\frac{e^{-\mu_a^2/\alpha_a}}{(\pi\alpha_a)^{1/2}}\right]\mu_{a_1}\cdots\mu_{a_l}. \end{aligned} \tag{14}$$

The integral in (14) will be zero unless the indices $a_1,\ldots,a_l$ appear in pairs, quadruples, etc., so that l must be even. We therefore rewrite (14) as

$$K(\mathbf{R}) = \frac{1}{2}\sum_{I\neq J}\sum_{l=0}^{\infty}\frac{1}{(2l)!}\frac{\partial^{2l}\phi(\mathbf{R}_I-\mathbf{R}_J)}{\partial x_{\gamma_1}\cdots\partial x_{\gamma_{2l}}} \times(U_{I\gamma_1,a_1}-U_{J\gamma_1,a_1})\cdots(U_{I\gamma_{2l},a_{2l}}-U_{J\gamma_{2l},a_{2l}}) \times\int d^{3N}\mu\left[\frac{e^{-\mu_a^2/\alpha_a}}{(\pi\alpha_a)^{1/2}}\right]\mu_{a_1}\cdots\mu_{a_{2l}}. \quad (15)$$

To evaluate

$$\int d^{3N}\mu\left[\frac{e^{-\mu_a^2/\alpha_a}}{(\pi\alpha_a)^{1/2}}\right]\mu_{a_1}\cdots\mu_{a_{2l}},$$

we use the pairing theorem,[2] which states that we sum over all possible ways of pairing the indices and that each term in this sum is then evaluated as if the pairs were independent (e.g., a quadruple is evaluated as two distinct pairs). For example, one possible pairing of indices is $a_{l+1}=a_1, a_{l+2}=a_2,\ldots,a_{2l}=a_l$, for which

$$\int d^{3N}\mu\left[\frac{e^{-\mu_a^2/\alpha_a}}{(\pi\alpha_a)^{1/2}}\right]\mu_{a_1}^2\cdots\mu_{a_l}^2=\frac{\alpha_{a_1}}{2}\frac{\alpha_{a_2}}{2}\cdots\frac{\alpha_{a_l}}{2}.$$

However, since (15) is symmetric with respect to exchanging indices, all different pairings give the same answer. Since there are $(2l-1)!!=(2l-1)(2l-3)\cdots(3)(1)$ different ways of pairing $a_1,\ldots,a_{2l}$, we have

$$K(\mathbf{R}) = \frac{1}{2}\sum_{I\neq J}\sum_{l=0}^{\infty}\frac{1}{(2l)!}\frac{\partial^{2l}\phi(\mathbf{R}_I-\mathbf{R}_J)}{\partial x_{\gamma_1}\cdots\partial x_{\gamma_{2l}}}(2l-1)!! \times(U_{I\gamma_1,a_1}-U_{J\gamma_1,a_1})\frac{\alpha_{a_1}}{2}(U_{I\gamma_2,a_1}-U_{J\gamma_2,a_1})\cdots \times(U_{I\gamma_{2l-1},a_l}-U_{J\gamma_{2l-1},a_l})\frac{\alpha_{a_l}}{2}(U_{I\gamma_{2l},a_l}-U_{J\gamma_{2l},a_l}).$$

Noting that $(2l-1)!!/(2l)!=1/2^l l!$ and defining

$$\left(D^{IJ}\right)_{\alpha\beta}=(U_{I\alpha,a}-U_{J\alpha,a})\alpha_a(U_{I\beta,a}-U_{J\beta,a}), \quad (16)$$

we have

$$K(\mathbf{R}) = \frac{1}{2}\sum_{I\neq J}\sum_{l=0}^{\infty}\frac{1}{l!}\frac{\partial^{2l}\phi(\mathbf{R}_I-\mathbf{R}_J)}{\partial x_{\gamma_1}\cdots\partial x_{\gamma_{2l}}} \times\left(\frac{D^{IJ}}{4}\right)_{\gamma_1\gamma_2}\cdots\left(\frac{D^{IJ}}{4}\right)_{\gamma_{2l-1}\gamma_{2l}}. \quad (17)$$

In the literature up to now,[6,15] this Taylor expansion has been truncated. Furthermore, after the truncation, the expression is expanded about equilibrium. Terms in this double expansion are grouped together according to powers of a quantum smallness parameter, essentially the equilibrium value of D^{IJ}. The nomenclature "nth-order EPMC" means the results obtained by truncating at $l=n$, expanding about equilibrium, and only keeping terms of order $(D^{IJ})^n$. This procedure quickly becomes prohibitive. At finite temperature, nothing higher than a second-order EPMC simulation is manageable. At zero temperature, an inconsistent third-order EPMC calculation is possible. Most applications of EPMC theory to crystals have stopped at first order.[6] This is acceptable only for the heavier crystals. Liu *et al.*[15] have presented a second-order calculation for both argon and neon, and a third-order, zero-temperature calculation for neon. If we define a (temperature-dependent) convergence parameter as the ratio (at equilibrium) between the second-order term and the first-order term in (17), we find that,[15] for low-temperature neon, this parameter is as high as 0.8. Thus the validity of this entire expansion procedure is questionable.

However, it is not necessary to expand (17) about equilibrium, nor to truncate it, as the infinite series can, in fact, be summed analytically. Fourier transforming $\phi(\mathbf{x})$ in (17), we have

$$\phi(\mathbf{x})=\left(\frac{1}{2\pi}\right)^3\int d^3q\,\tilde{\phi}(\mathbf{q})e^{i\mathbf{q}\cdot\mathbf{x}},$$

$$K(\mathbf{R}) = \frac{1}{2}\sum_{I\neq J}\left(\frac{1}{2\pi}\right)^3\int d^3q\,\tilde{\phi}(\mathbf{q})\sum_{l=0}^{\infty}\frac{1}{l!}(iq_{\gamma_1})\cdots(iq_{\gamma_{2l}}) \times e^{i\mathbf{q}\cdot(\mathbf{R}_I-\mathbf{R}_J)}\left(\frac{D^{IJ}}{4}\right)_{\gamma_1\gamma_2}\cdots\left(\frac{D^{IJ}}{4}\right)_{\gamma_{2l-1}\gamma_{2l}}.$$

Inverse transforming $\tilde{\phi}(\mathbf{q})$ and assuming D^{IJ} positive definite,

$$\begin{aligned}K(\mathbf{R}) &= \frac{1}{2}\sum_{I\neq J}\left(\frac{1}{2\pi}\right)^3\int d^3x\,\phi(\mathbf{x})\int d^3q\,e^{-i\mathbf{q}\cdot\mathbf{x}} \times e^{i\mathbf{q}\cdot(\mathbf{R}_I-\mathbf{R}_J)}\sum_{l=0}^{\infty}\frac{1}{l!}\left(-\mathbf{q}^T\frac{D^{IJ}}{4}\mathbf{q}\right)^l \\ &= \frac{1}{2}\sum_{I\neq J}\left(\frac{1}{2\pi}\right)^3\int d^3x\,\phi(\mathbf{x}) \times\int d^3q\,e^{-\mathbf{q}^T D^{IJ}\mathbf{q}+i\mathbf{q}\cdot(\mathbf{R}_I-\mathbf{R}_J-\mathbf{x})} \\ &= \frac{1}{2}\sum_{I\neq J}\left(\frac{1}{2\pi}\right)^3\int d^3x\,\phi(\mathbf{x})\frac{(4\pi)^{3/2}}{(\det D^{IJ})^{1/2}} \times e^{-(\mathbf{R}_I-\mathbf{R}_J-\mathbf{x})^T\left(D^{IJ}\right)^{-1}(\mathbf{R}_I-\mathbf{R}_J-\mathbf{x})} \\ &= \frac{1}{2}\sum_{I\neq J}\int d^3x\,\frac{e^{-\mathbf{x}^T\left(D^{IJ}\right)^{-1}\mathbf{x}}}{(\pi^3\det D^{IJ})^{1/2}} \times\phi(\mathbf{R}_I-\mathbf{R}_J+\mathbf{x}). \quad (18)\end{aligned}$$

We call this simply the EPMC method, as opposed to the finite-order EPMC method (e.g., a second-order EPMC method).

Bringing together Eqs. (4), (5), (9), (10), (11), (12), (16), and (18) as a convenient reference, we have

$$Z_0=\left(\frac{m}{2\pi\beta\hbar^2}\right)^{3N/2}\int d^{3N}R\,e^{-\beta V_{\rm eff}(\mathbf{R})},$$

$$V_{\rm eff}(\mathbf{R})=K(\mathbf{R})-\frac{m\alpha_a f_a^2}{\beta^2\hbar^2}+\frac{1}{\beta}\sum_a\ln\left(\frac{\sinh f_a}{f_a}\right),$$

$$K(\mathbf{R}) = \frac{1}{2}\sum_I\sum_{J\neq I}\int d^3x\,\frac{e^{-\mathbf{x}^T[D^{IJ}]^{-1}\mathbf{x}}}{(\pi^3\det D^{IJ})^{1/2}} \times\phi(\mathbf{R}_I-\mathbf{R}_J+\mathbf{x}),$$

$$
\begin{aligned}
\left(D^{IJ}\right)_{\alpha\beta} &= (U_{I\alpha,a} - U_{J\alpha,a})\alpha_a(U_{I\beta,a} - U_{J\beta,a}),\\
\alpha_a &= \frac{\beta\hbar^2}{2mf_a}\left(\coth f_a - \frac{1}{f_a}\right),\\
f_a &= \frac{\beta\hbar\omega_a}{2},\\
U^T_{ai}\tilde{K}_{ij}U_{jb} &= m\omega_a^2\delta_{ab},\\
\tilde{K}_{I\alpha,J\beta} &= \frac{\partial^2 K(\mathbf{R})}{\partial R_{I\alpha}\partial R_{J\beta}}.
\end{aligned}
\tag{19}
$$

It is worthwhile comparing this result to first-order self-consistent phonon theory[3] (SC1). The SC1 equations are evaluated at the equilibrium positions and thus great simplification is achieved by going to phonon coordinates. For comparison purposes, however, we shall *not* do this:

$$
\begin{aligned}
F_{\mathrm{SC1}} &= K(\mathbf{R}) - \frac{1}{2\beta}f_a\coth f_a + \frac{1}{\beta}\sum_a \ln(2\sinh f_a),\\
K(\mathbf{R}) &= \frac{1}{2}\sum_I\sum_{J\neq I}\int d^3x\,\frac{e^{-\mathbf{x}^T[D^{IJ}]^{-1}\mathbf{x}}}{(\pi^3\det D^{IJ})^{1/2}}\\
&\quad\times\phi(\mathbf{R}_I - \mathbf{R}_J + \mathbf{x}),\\
\left(D^{IJ}\right)_{\alpha\beta} &= (U_{I\alpha,a} - U_{J\alpha,a})\alpha_a(U_{I\beta,a} - U_{J\beta,a}),\\
\alpha'_a &= \frac{\beta\hbar^2}{2mf_a}\coth f_a,\\
f_a &= \frac{\beta\hbar\omega_a}{2},\\
U^T_{ai}\tilde{K}_{ij}U_{jb} &= m\omega_a^2\delta_{ab},\\
\tilde{K}_{I\alpha,J\beta} &= \frac{\partial^2 K(\mathbf{R})}{\partial R_{I\alpha}\partial R_{J\beta}}.
\end{aligned}
\tag{20}
$$

We see that in many respects, the EPMC and SC1 theories are identical. We wish to point out the differences. Both EPMC and SC1 theories simulate particle fluctuations about a given configuration by smearing the potential. The smearing is Gaussian and the width is governed by α. We notice that the EPMC value of α is just the quantum mechanical portion of the SC1 value of α, i.e., α_{SC1} minus its classical limit. Comparing F_{SC1} with V_{eff}, we notice the same thing among the phonon terms. The physical picture of the EPMC theory that emerges is that the contributions to the free energy from the particle fluctuations are evaluated by separating the quantum fluctuations from the classical ones. The quantum fluctuations effectively smear the potential and also contribute to the kinetic energy (the phonon terms). These two contributions are approximated by choosing (variationally) the best possible harmonic oscillator force constants that will reproduce these. The contributions from the classical fluctuations are not approximated, leaving the partition function in its classical, integral form. It is important to realize that, since the phonon modes only represent the quantum vibrations of the system, these are not the observable phonon modes, such as in SC1 theory where the phonon modes come from the entire fluctuations.

At zero temperature, the quantum fluctuations represent the full fluctuations, so that the EPMC and SC1 theories are identical. In the classical limit, where there are no quantum fluctuations, the EPMC theory is exact. In fact,

$$
\begin{aligned}
V_{\mathrm{eff}}(\mathbf{R}) &\to K(\mathbf{R}) + O(\hbar^4)\\
&= V(\mathbf{R}) + \frac{\beta\hbar^2}{24m}\nabla^2 V(\mathbf{R}) + O(\hbar^4)
\end{aligned}
\tag{21}
$$

[where $V(\mathbf{R})$ is the two-body potential (13)], so that the EPMC theory reproduces the first term of the Wigner expansion.[1] Notice that the first term of the Wigner expansion is isotropic, so that even with an isotropic approximation, the EPMC theory reproduces it. The SC1 theory, on the other hand, becomes unreliable at higher temperatures since the full fluctuations become too large to be well approximated by Gaussian smearing. Hence, the EPMC and SC1 theories are identical at $T = 0$, but the SC1 theory progressively gets less reliable as the temperature increases whereas the EPMC theory progressively gets more reliable until it becomes exact. Thus, in principle, the EPMC theory is inherently superior to the SC1 theory.

There is one important difference between the SC1 and EPMC theories with a serious consequence. Since the SC1 theory approximates the full fluctuations, the SC1 equations (20) need only be solved once (at equilibrium). This involves a first guess for U and ω, getting K, getting a new U and ω, ..., and iterating until convergence. However, in the EPMC method, this SC1-like iteration procedure must be done at *every* $\mathbf{R}$ (furthermore without the simplifications of phonon modes). This would make the Monte Carlo evaluation extremely long. Every iteration at fixed $\mathbf{R}$ involves diagonalization, which is a process of order N^3 since we cannot go to phonon coordinates (in which case it would be of order N). This is an extremely large workload; it takes of order 1 min for 125 atoms on a Sparcstation 2. Thus, every Monte Carlo move requires several minutes. Getting a well converged energy (for example) would require tens of thousands of hours. A simplifying approximation is necessary to make EPMC simulations practical. In the low-coupling approximation[16] (LCA), changes in α and U [in (19)] from equilibrium are assumed to be negligible. D^{IJ} therefore remains unchanged, as do the phonon terms in V_{eff}. Hence, as $\mathbf{R}$ changes, the only changes to $V_{\mathrm{eff}}(\mathbf{R})$ come from the $\mathbf{R}$ dependence of $V(\mathbf{R})$. Neither D^{IJ} nor the phonon terms in V_{eff} need be recalculated. This is attractive because the iterative procedure need only be done once, at equilibrium. Thus, classical Monte Carlo simulations become an efficient way of evaluating the partition function. At zero temperature, only the equilibrium configuration contributes to the free energy since classically the atoms do not fluctuate about equilibrium. Therefore, the LCA is exact at $T = 0$. We also note that assuming the LCA does not change the result (21) since (21) has no phonon dependence. Therefore, the LCA is also exact in the classical limit and in the first term of the Wigner expansion. The hope is that, since it is exact at both temperature extremes, it is rather good in between. If this is not the case (so that the LCA must be abandoned) then one may as well use the PIMC

method, since the EPMC method without the LCA takes too much computer time.

Last, we note that the effective potential is volume and temperature dependent. This means that we must be careful when taking derivatives of the partition function. For example, we have

$$E = -\frac{\partial}{\partial\beta}\ln Z_0 = \frac{3N}{2\beta} + \langle V_{\rm eff}\rangle_0 + \beta\left\langle \frac{\partial}{\partial\beta}V_{\rm eff}\right\rangle_0, \quad (22)$$

$$P = \frac{1}{\beta}\frac{\partial}{\partial V}\ln Z_0 = \frac{N}{\beta V} - \left\langle \frac{\partial}{\partial V}V_{\rm eff}\right\rangle,$$

$$C_V = \left(\frac{\partial E}{\partial T}\right)_V = \frac{3Nk}{2} - k\beta^2\left\langle 2\frac{\partial V_{\rm eff}}{\partial\beta} + \beta\frac{\partial^2 V_{\rm eff}}{\partial\beta^2}\right\rangle + k\beta^2\left\{\left\langle\left(V_{\rm eff}+\beta\frac{\partial V_{\rm eff}}{\partial\beta}\right)^2\right\rangle - \left\langle V_{\rm eff}+\beta\frac{\partial V_{\rm eff}}{\partial\beta}\right\rangle^2\right\},$$

$$B = -V\left(\frac{\partial P}{\partial V}\right)_T = \frac{N}{\beta V} + V\left\langle\frac{\partial^2 V_{\rm eff}}{\partial V^2}\right\rangle - \beta V\left\{\left\langle\left(\frac{\partial}{\partial V}V_{\rm eff}\right)^2\right\rangle - \left\langle\frac{\partial}{\partial V}V_{\rm eff}\right\rangle^2\right\}.$$

We also explicitly see here how the specific heat and bulk modulus depend on fluctuations, which makes these quantities difficult to calculate accurately.

III. COMPUTATIONAL DETAILS

From a computational point of view, the EPMC method with the LCA is very easy to program. In the LCA, the phonon terms are independent of $\mathbf{R}$ and are equal to their equilibrium values. If we let

$$\mathcal{W} = \frac{1}{\beta}\sum_a \ln\left(\frac{\sinh f_a}{f_a}\right) - \frac{m\alpha_a f_a^2}{\beta^2\hbar^2},$$

then we may rewrite (9) as

$$Z_0 = \left(\frac{m}{2\pi\beta\hbar^2}\right)^{3N/2} e^{-\beta\mathcal{W}}\int d^{3N}R\, e^{-\beta K(\mathbf{R})}.$$

We calculate $\mathcal{W}$ only once, as well as its temperature and volume derivatives, which are evaluated numerically. For example, the energy (22) can be rewritten as

$$E = \frac{3N}{2\beta} + \mathcal{W} + \beta\frac{\partial\mathcal{W}}{\partial\beta} + \langle K\rangle_0 + \beta\left\langle\frac{\partial K}{\partial\beta}\right\rangle_0, \quad (23)$$

with similar decompositions for the pressure, specific heat, and bulk modulus. We rewrite K [Eq. (18)] as

$$K(\mathbf{R}) = \int\frac{d^3x}{\pi^{3/2}}e^{-\mathbf{x}^2}\phi(\mathbf{R}_I - \mathbf{R}_J + U^{IJ}\mathbf{x}), \quad (24)$$

where we have defined

$$\left(U^{IJ}\right)_{\alpha\beta} = V_{\alpha\beta}\sqrt{\Lambda_\beta},$$
$$V^T_{\alpha\gamma}\left(D^{IJ}\right)_{\gamma\delta}V_{\delta\beta} = \Lambda_\alpha\delta_{\alpha\beta}.$$

From (19), we see that D^{IJ} depends explicitly on β through α_a and f_a, and implicitly on β, V through ω_a and U_{ia}. Therefore, temperature and volume derivatives of K must include derivatives of U^{IJ}. For example,

$$\frac{\partial K}{\partial\beta} = \int\frac{d^3x}{\pi^{3/2}}e^{-\mathbf{x}^2}\left.\frac{\partial\phi(\mathbf{y})}{\partial y_\alpha}\right|_{\mathbf{y}=\mathbf{R}_I-\mathbf{R}_J+U\mathbf{x}}\frac{\partial}{\partial\beta}\left(U^{IJ}\right)_{\alpha\beta}x_\beta.$$

Since D^{IJ} is independent of $\mathbf{R}$ (in the LCA), U^{IJ} is evaluated once at equilibrium, as well as its derivatives, which are calculated numerically. With the LCA, one must never ignore the implicit dependence on β, V (as could be done for first derivatives *without* the LCA, since the variational procedure assures us that $\delta V_{\rm eff}/\delta\omega_a = \delta V_{\rm eff}/\delta U_{ia} = 0$). Also note that taking the numerical derivative of the eigenvalues and eigenvectors of a matrix is tricky because these are not unique (change order of eigenvalues, multiply eigenvector by -1, linear combinations of eigenvectors for degenerate eigenvalues). Imagine, for example, evaluating a particular eigenvector V, increasing the temperature infinitesimally, and reevaluating the same eigenvector V'. We expect $V' = V + \delta V$. However, since both evaluations are numerical, we may get $V' = -V - \delta V$, since both V' and $-V'$ are solutions. Taking $\partial V/\partial\beta = (V' - V)/\delta\beta$ would be disastrous. The diagonalization algorithm must be designed to always return a unique answer.

The Gaussian smearing (24) can be evaluated simply by Gauss-Hermite integration. An n-point Gauss-Hermite integration is a numerical procedure where

$$\int_{-\infty}^{\infty} f(x)e^{-x^2}dx \approx \sum_{i=1}^{n} w_i f(x_i).$$

The weights w_i and the points x_i (zeros of Hermite polynomials) are tabulated in Ref. 19 for various values of n. The three-dimensional Gauss-Hermite integration is evaluated as a series of one-dimensional integrations:

$$\int_{-\infty}^{\infty} f(\mathbf{x})e^{-\mathbf{x}^2}d^3x \approx \sum_{i_1,i_2,i_3=1}^{n} w_{i_1}w_{i_2}w_{i_3}f(x_{i_1},x_{i_2},x_{i_3}).$$

These Gauss-Hermite integrations vectorize well and each pair contribution to the smeared potential can be done in parallel, so that many high-performance computing platforms are available. Our program ran on a vector supercomputer, the Cray C-90. We did not parallelize our code. As evidence for how well this algorithm vectorizes, our code ran at 500 Mflop on one processor of the C-90, while the theoretical peak performance is 1 Gflop. The time required for the code to run depends on how many points are used in this integration. One point would correspond (in speed and in result) to a classical Monte Carlo calculation (one evaluation of the potential per move). The first quantum correction comes from two points, requiring eight potential evaluations per move (two cubed, since there are three dimensions). The number of points can be chosen to be the smallest allowable such that the systematic error caused by using a small number of points is less than the expected statistical error from the Monte Carlo simulation.

Here we see why the isotropic approximation can be so attractive. In a fully isotropic crystal, a six-point integration would require only 6 potential evaluations per move rather than 216, since there is effectively only one dimension. Similarly, separating the transverse and longitudinal modes would effectively give a two-dimensional problem, requiring 36 potential evaluations per move. However, for a two-point integration, the gain in speed would only be a factor of 4.

We also note that the EPMC method using an n-point Gauss-Hermite integration is more accurate than an $(n-1)$th-order EPMC simulation and probably more accurate than an nth-order EPMC simulation [recall the finite-order approximation scheme (17)]. The n-point Gauss-Hermite integration is exact for polynomials of order $2n-1$. In the nth-order EPMC method, we start by expanding $V(\mathbf{R}+U\boldsymbol{\mu})$ in (8) around $\mathbf{R}$ up to order $2n$ and discard the rest [equivalent to stopping at $l=n$ in (17)]. Imagine we use this polynomial potential of order $2n$ instead of the real potential. This will give identical results in the nth-order EPMC method. But with an $(n+1)$-point Gauss-Hermite integration, we would get exact results. Since the nth-order EPMC method would further approximate this polynomial potential by expanding around equilibrium, then the $(n+1)$-point Gauss-Hermite integration is definitely more accurate than the nth-order EPMC method. However, with the Gauss-Hermite integration, we do not have a polynomial potential; we have the full potential, which we can think of as an infinite-order polynomial. Therefore, an n-point Gauss-Hermite integration will get the exact contribution from the first $(2n-1)$th-order terms, and an approximate contribution from $(2n)$th-order and all higher-order terms. This is compared with the nth-order EPMC method which will *approximate* the first $(2n-1)$th-order terms, also approximate the $(2n)$th-order term, and *leave out* all higher-order terms. It therefore seems reasonable to state that an n-point Gauss-Hermite integration is more accurate than an nth-order EPMC method.

IV. RESULTS

Neon is a particularly suitable test of any theory because its zero-point motion is so large. In fact, perturbation theory does not converge for neon at any temperature. We have calculated the zero-pressure nearest-neighbor distance, internal energy, isochoric specific heat, and isothermal bulk modulus[20] for a model of the isotope Ne.[22] These were evaluated by averaging analytical expressions rather than taking numerical derivatives. The model used was a nearest-neighbor Lennard-Jones potential of the form

$$\phi(\mathbf{x}) = 4\epsilon\left[\left(\frac{\sigma}{r}\right)^{12} - \left(\frac{\sigma}{r}\right)^{6}\right], \tag{25}$$

where $r=|\mathbf{x}|$. The reason for this was to make contact with the work of Liu *et al.*[15] The potential parameters appropriate to solid neon are listed in Table I. We compare our results with the second-order EPMC method (and third order at $T=0$), with the SC1 method, and with the first-order Wigner expansion (avoiding a comparison with classical Monte Carlo simulation because, even near melting, neon is too far from being a classical solid). Results for the first-order Wigner expansion were calculated simply by replacing V_{eff} with Eq. (21) in the Monte Carlo simulation.

TABLE I. Parameters[a] for the Lennard-Jones potential (Eq. 25).

ϵ (10^{-16} ergs)	σ (10^{-8} cm)
72.09	2.7012

[a]Taken from Ref. 15.

We used a six-point Gauss-Hermite integration. This ensured that any errors from the numerical integration were about an order of magnitude smaller than the statistical uncertainty in the energy. We used 125 atoms in an oblique box with periodic boundary conditions. At the start of the run, all atoms were positioned at the equilibrium sites of a fcc lattice. We generated 8×10^6 single-particle moves using standard METROPOLIS sampling and discarded the first 10^6 to thermalize the system. Every 125th move was saved to contribute to averages; variances were calculated by the "blocking method."[20] The single-particle move size was adjusted to give approximately a 50% acceptance rate. The time required for one such run was about 2 h on one processor of a Cray C-90. Several short runs (10 min) at constant tem-

TABLE II. EPMC data. T is the temperature and d is the nearest-neighbor distance at which the pressure P, the internal energy E, the specific heat C_V, and the bulk modulus B were calculated. Adjusted d is the value of the nearest-neighbor distance which adjusts the pressure to zero using the bulk modulus. It is useful to note that $\epsilon/k = 52.2\,\text{K}$ and that $\epsilon/\sigma^3 = 36.6\,\text{MPa}$.

T (ϵ/k)	d (σ)	P (ϵ/σ^3)	E ($N\epsilon$)	C_V (Nk)	B (ϵ/σ^3)	Adjusted d (σ)
0.000	1.166376	0.0000 ± 0.0000	-4.39867 ± 0.00000	0.00 ± 0.00	28.19 ± 0.00	1.166376 ± 0.000000
0.019	1.166378	0.0004 ± 0.0001	-4.39831 ± 0.00003	0.03 ± 0.02	28.19 ± 0.01	1.166384 ± 0.000002
0.038	1.166380	0.0008 ± 0.0002	-4.39790 ± 0.00007	0.02 ± 0.03	28.19 ± 0.02	1.166391 ± 0.000003
0.057	1.166417	0.0000 ± 0.0005	-4.39707 ± 0.00013	0.01 ± 0.02	28.20 ± 0.02	1.166418 ± 0.000007
0.096	1.166525	0.0017 ± 0.0006	-4.39351 ± 0.00018	0.14 ± 0.03	28.05 ± 0.05	1.166548 ± 0.000009
0.134	1.166894	-0.0024 ± 0.0012	-4.38491 ± 0.00032	0.34 ± 0.03	27.67 ± 0.06	1.166860 ± 0.000017
0.172	1.167483	0.0025 ± 0.0013	-4.36689 ± 0.00035	0.66 ± 0.03	26.86 ± 0.09	1.167518 ± 0.000019
0.211	1.168495	0.0003 ± 0.0016	-4.33930 ± 0.00044	0.89 ± 0.03	26.10 ± 0.10	1.168499 ± 0.000025
0.249	1.170053	0.0008 ± 0.0020	-4.29689 ± 0.00052	1.19 ± 0.03	24.72 ± 0.13	1.170066 ± 0.000031
0.287	1.172137	0.0006 ± 0.0029	-4.24160 ± 0.00076	1.43 ± 0.03	23.28 ± 0.14	1.172147 ± 0.000049
0.326	1.174744	-0.0033 ± 0.0026	-4.17483 ± 0.00066	1.62 ± 0.03	21.66 ± 0.19	1.174684 ± 0.000047
0.364	1.177736	-0.0004 ± 0.0029	-4.09675 ± 0.00074	1.82 ± 0.03	19.77 ± 0.19	1.177729 ± 0.000058
0.402	1.181365	-0.0013 ± 0.0041	-4.00690 ± 0.00099	1.94 ± 0.03	18.12 ± 0.21	1.181337 ± 0.000090
0.421	1.183417	0.0022 ± 0.0035	-3.95642 ± 0.00088	1.98 ± 0.03	17.24 ± 0.23	1.183468 ± 0.000081
0.440	1.185725	-0.0029 ± 0.0034	-3.90369 ± 0.00088	2.06 ± 0.03	16.10 ± 0.24	1.185654 ± 0.000085

perature were usually needed to approximately zero the pressure prior to the full run. All our results are shown in Table II.

Figure 1 shows the zero-pressure nearest-neighbor distance as a function of temperature. Our EPMC distance was adjusted to zero pressure since we have available the volume dependence of the pressure, i.e., the bulk modulus. The error bars are too small to be shown. Some general remarks are in order. We have stated that the EPMC theory coincides with the SC1 theory at $T = 0$, but that the SC1 theory becomes less reliable as the temperature increases, whereas the EPMC theory becomes more reliable, reproducing the first Wigner term and becoming exact in the classical limit. This is evident from the plot where at $T = 0$, the EPMC and SC1 results are identical, and as the temperature increases, the EPMC result approaches the results of the first-order Wigner expansion, interpolating between the quantum regime and the classical regime. This is one of the EPMC theory's great qualities.

The difference between the results of Liu *et al.*[15] and our own can only be due to the finite-order (second-order) EPMC method and to the isotropic approximation made in this earlier work. Two features strike us. First is that the third-order, zero-temperature nearest-neighbor distance of Liu *et al.* is off by more than 5% of the total expansion neon undergoes from $T = 0$ to melting. Second, we notice that the second-order results give a negative thermal expansion. Since the change in nearest-neighbor distance between the second-order and third-order EPMC results is small, it is reasonable to believe that the third-order, zero-temperature nearest-neighbor distance is well converged. Hence, the only possible source for the large discrepancy between our EPMC results and the third-order EPMC results of Liu *et al.* is the isotropic approximation. We therefore ran an isotropic version of our program. Results are presented in Table III. This verified that the isotropic approximation is responsible for the error in the third-order equilibrium distance. It is *not* a valid approximation. Also, Liu *et al.* have concluded that the negative thermal expansion is due to the terminated expansion (17). This is suggested by the observation that the third-order point reduces the negative thermal expansion; more compelling evidence can be found in Ref. 15 by comparing the first-order curve, where the negative thermal expansion is very large, to the second-order curve, where it has been greatly reduced. However, the conclusion of Liu *et al.* is not completely correct. The isotropic approximation itself causes a small negative thermal expansion, as can be seen by our isotropic data. This is unexpected because it would seem that there is no reason for the isotropy approximation to cause a negative thermal expansion.

The second-order EPMC results approach ours at the higher temperatures since both are exact in the classical limit and in the first Wigner term. The quantum effects in neon are so large that, even at the highest temperatures we considered, there is still quite a large discrepancy between the first-order Wigner expansion and the EPMC results, and at lower temperatures the Wigner expansion, as expected, breaks down.

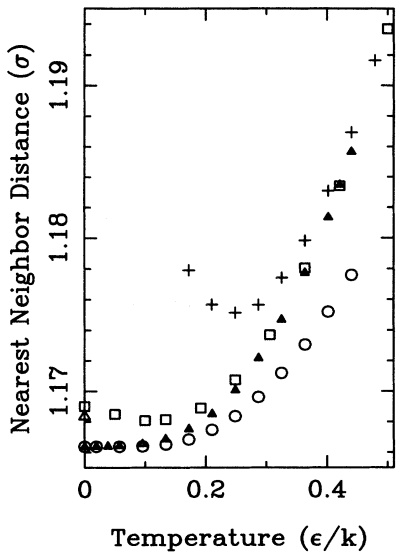

FIG. 1. Nearest-neighbor distance at zero pressure versus temperature. Solid triangles are EPMC, open squares are second-order EPMC, the open triangle is third-order EPMC, open circles are SC1, and crosses are first-order Wigner expansion results.

In Fig. 2, the internal energy is plotted versus temperature; the error bars are again too small to be shown. Keeping in mind the discrepancies in the previous comparison, we were at first surprised to see such good agreement. However, this is due to fortuitous cancellation of errors: the error caused by neglecting third-order EPMC corrections and the error caused by the isotropic approximation. This is verified by looking at the better-converged third-order point and at our own isotropic data. If Liu *et al.* had not assumed an isotropic crystal, their second-order energy would have been far below ours, and their third-order point would have brought it into better agreement with ours.

Figure 3 shows the isochoric specific heat as a function of temperature. The second-order data were taken from Ref. 21. The cancellation of errors which led to a better-than-expected agreement between our results for the energy and the second-order energy occurs again for the specific heat. The error bars are not shown because the clutter would make the plot too difficult to read, but they are approximately the size of the graph symbols. They are much larger than the energy's error bars. An accurate calculation of the specific heat is difficult because it

TABLE III. Isotropic EPMC data. Symbols as in Table II.

T (ϵ/k)	d (σ)	P (ϵ/σ^3)	E ($N\epsilon$)	C_V (Nk)	B (ϵ/σ^3)	Adjusted d (σ)
0.000	1.168057	0.0000 ± 0.0000	-4.3647 ± 0.0000	0.00 ± 0.00	27.67 ± 0.00	1.168057 ± 0.000000
0.057	1.167945	0.0001 ± 0.0004	-4.3632 ± 0.0001	0.06 ± 0.03	27.73 ± 0.02	1.167947 ± 0.000006

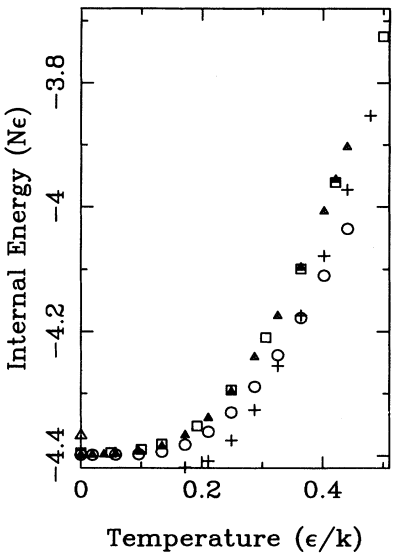

FIG. 2. Internal energy at zero pressure versus temperature. Notation as in Fig. 1.

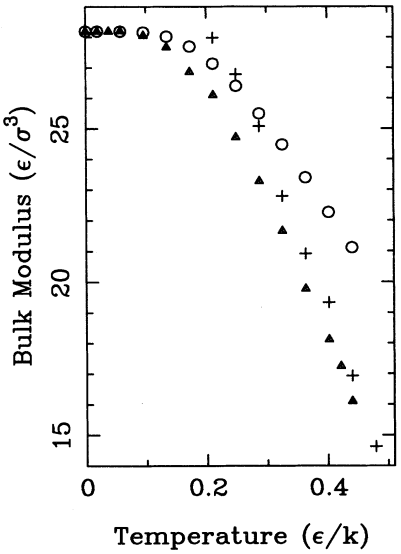

FIG. 4. Bulk modulus at zero pressure versus temperature. Notation as in Fig. 1.

depends on the fluctuation of the energy. Reducing the error bars by about a factor of 10, thus reducing them to the same relative size as the energy's error bars (ignoring the energy's large negative constant), would require on the order of 1×10^9 moves (about a factor of 100 longer).

In Fig. 4, we present the first EPMC calculation of the isothermal bulk modulus. There are no second-order EPMC results for the bulk modulus, but we would expect to see a maximum at low temperature since the nearest-neighbor distance had a minimum (this is true of our isotropic data). The effect of the isotropic approximation is again to cause a large systematic error at low temperatures. The bulk modulus is related to the fluctuation of the pressure, and so it is also a difficult quantity to calculate accurately. The error bars, again not drawn for clarity, are approximately the size of the graph symbols, although somewhat smaller at lower temperatures and larger at higher temperatures. We also note that the SC1 results are in serious disagreement with the EPMC method, except at low temperature.

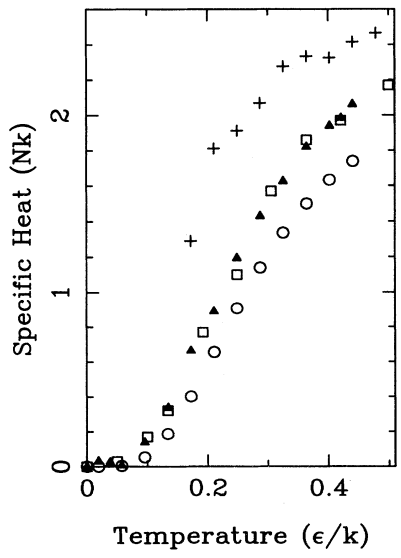

FIG. 3. Constant volume specific heat at zero pressure versus temperature. Notation as in Fig. 1.

It is clear that there is no longer any reason to use the finite-order EPMC method (and certainly not the isotropic approximation). The formulation of the three-dimensional EPMC theory presented here, even with only a two-point Gaussian smearing, is decisively superior to all previous formulations; their use is now obsolete. The EPMC method is the best available alternative to the PIMC method; it is much faster and is accurate over the entire temperature range of the crystal. However, despite the successes of this formulation of EPMC theory, we have discovered some fundamental difficulties that appear in crystals with large zero-point energies. We plan to discuss these problems in a subsequent paper.

We believe that this formalism is applicable to all condensed systems, whether crystalline, amorphous, or liquid, and that it holds at all temperatures. There may be concern that some of the frequencies defined in Eq. (3) can be imaginary, a point that has been noted by previous authors.[17] However, the physically important quantities are the functions α, defined in Eq. (4), and these are always positive.

ACKNOWLEDGMENTS

We would like to thank Dr. E. Freidkin, Dr. A. A. Maradudin, and Dr. V. Tognetti for their helpful comments. This work was partially supported by the U.S. National Science Foundation under Grant No. DMR92-02907 and by the Pittsburgh Supercomputing Center under Grant No. DMR93-0035P.

[1] E. P. Wigner, Phys. Rev. **40**, 749 (1932); K. İmre, E. Özizmir, M. Rosenbaum, and P. F. Zweifel, J. Math. Phys. **8**, 1097 (1967).
[2] T. H. K. Barron and M. L. Klein, in *Dynamical Properties of Solids*, edited by G. K. Horton and A. A. Maradudin (North-Holland, Amsterdam, 1974), Vol. 1.
[3] N. S. Gillis, N. R. Werthamer, and T. R. Koehler, Phys. Rev. **165**, 951 (1968).
[4] K. E. Schmidt and D. M. Ceperly, in *The Monte Carlo Method in Condensed Matter Physics*, edited by K. Binder (Springer-Verlag, Berlin, 1992); A. R. McGurn, in *Dynamical Properties of Solids*, edited by G. K. Horton and A. A. Maradudin (North-Holland, Amsterdam, 1995), Vol. 7.
[5] R. P. Feynman, *Statistical Mechanics* (Benjamin, Reading, MA, 1972).
[6] A. Cuccoli, A. Macchi, V. Tognetti, and R. Vaia, Phys. Rev. B **47**, 14923 (1993).
[7] S. Liu, G. K. Horton, E. R. Cowley, A. R. McGurn, A. A. Maradudin, and R. F. Wallis, Phys. Rev. B **45**, 9716 (1992).
[8] E. L. Pollock and D. M. Ceperley, Phys. Rev. B **30**, 2555 (1984).
[9] P. Whitlock and R. M. Panoff, Can. J. Phys. **65**, 1409 (1987).
[10] T. Macfarland, G. V. Chester, M. H. Kalos, L. Reatto, and S. A. Vitiello, Physica B **194-196**, 525 (1994).
[11] R. Giachetti and V. Tognetti, Phys. Rev. Lett. **55**, 912 (1985); Phys. Rev. B **33**, 7647 (1986).
[12] R. P. Feynman and H. Kleinert, Phys. Rev. A **34**, 5080 (1986).
[13] S. Srivastava and Vishwamittar, Phys. Rev. A **44**, 8006 (1991).
[14] A. Cuccoli, V. Tognetti, and R. Vaia, Phys. Rev. B **41**, 9588 (1990).
[15] S. Liu, G. K. Horton, and E. R. Cowley, Phys. Rev. B **44**, 11714 (1991).
[16] A. Cuccoli, A. Macchi, M. Neumann, V. Tognetti, and R. Vaia, Phys. Rev. B **45**, 2088 (1992).
[17] E. R. Cowley and G. K. Horton, in *Dynamical Properties of Solids*, edited by G. K. Horton and A. A. Maradudin (North-Holland, Amsterdam, 1995), Vol. 7.
[18] R. Peierls, Phys. Rev. **54**, 918 (1938).
[19] *Handbook of Mathematical Functions with Formulas, Graphs, and Mathematical Tables*, edited by M. Abramowitz and I. A. Stegun, Natl. Bur. Stand. Appl. Math. Ser. No. 55 (U.S. GPO, Washington, D.C., 1970).
[20] H. Flyvbjerg and H. G. Petersen, J. Chem. Phys. **91**, 461 (1989).
[21] S. Liu, Ph.D. thesis, Rutgers–the State University, 1991.